

Simulating net particle production and chiral magnetic current in a \mathcal{CP} -odd domain

Kenji Fukushima

Department of Physics, The University of Tokyo,
7-3-1 Hongo, Bunkyo-ku, Tokyo 113-0033, Japan

We elucidate the numerical formulation to simulate net production of particles and anomalous currents with \mathcal{CP} -breaking background fields which cause an imbalance between particles and anti-particles. For a concrete demonstration we numerically impose pulsed electric and magnetic fields to observe that the dynamical chiral magnetic current follows together with the net particle production. The produced particle density is quantitatively consistent with the axial anomaly, while the chiral magnetic current shows a delay before the onset, which leads to a suppression effect, and then approaches what is expected from the axial anomaly.

Introduction: In many quantum problems in physics it is highly demanded to establish a numerical framework to simulate full dynamical processes of particle production out of equilibrium. Unsettled and important problems include the leptogenesis and the baryogenesis for the explanation of the baryon asymmetry of the Universe (BAU). It is well-known that Sakharov's three conditions are needed for the BAU; namely, B -breaking process, \mathcal{C} and \mathcal{CP} violation, and out-of-equilibrium. The particle production on top of the electroweak sphaleron [1] accommodates a process with $\Delta(B+L) \neq 0$, which means that $B+L$ decays toward chemical-equilibrium [and this is why the idea based on the SU(5) grand unified theory [2] does not work out for the BAU]. Therefore, if the leptogenesis with some $(B-L)$ -breaking process beyond the Standard Model (see Ref. [3] for example) generates $L \neq 0$ initially, it would amount to $B \neq 0$ finally in chemical-equilibrium. The particle production associated with the sphaleron transition has a character of topological invariance and the index theorem relates the topological number to the change in the particle number. We must recall, however, that the sphaleron is a special static configuration at saddle-point and for general gauge configurations with \mathcal{C} and \mathcal{CP} violation we have to consider microscopic simulations with Weyl fermions.

The sphaleron transition rate is proportional to T^4 where T is the temperature [4], and so such topological fluctuations should be abundant also in the strong interaction when the physical system is heated up to $T > \Lambda_{\text{QCD}}$ as argued in Ref. [5]. Such high temperature is indeed realized in the quark-gluon plasma created in the relativistic heavy-ion collision (HIC) experiment. Although the strong interaction does not break \mathcal{CP} (except for negligibly small strong θ), we can still anticipate local violation of \mathcal{P} and \mathcal{CP} before thermalization [6]. This possibility is nowadays referred to commonly as the local parity violation (LPV). Theoretical and experimental challenges are still ongoing about the LPV detection. Along these lines the recognition of the interplay with pulsed magnetic field \mathbf{B} between two heavy ions was a major breakthrough [7]; \mathbf{B} on top of a \mathcal{CP} -odd domain would induce an electric current \mathbf{j} in parallel to \mathbf{B} , which

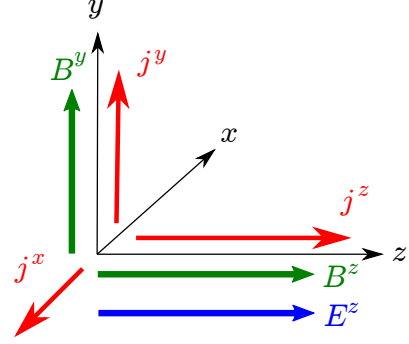


FIG. 1. Schematic view of currents induced by B_y in a \mathcal{CP} -odd domain realized by parallel E_z and B_z . The currents flow in all the x , y , and z directions; j_x is the Hall current and j_y is the CME current.

is summarized in a compact formula of the chiral magnetic effect (CME) with chiral chemical potential μ_5 [8]. In a realistic situation of the HIC we can anticipate \mathcal{P} and \mathcal{CP} violation not only from the QCD sphalerons but also from the glasma [9] which is a description of the initial condition of the HIC in terms of coherent fields. Then, without introducing μ_5 that has huge theoretical uncertainty (see Ref. [10] for a recent study with μ_5), we can and should directly compute the anomalous currents associated with the particle production in a \mathcal{CP} -odd domain with chromo-electric and chromo-magnetic fields [11].

It would be an intriguing attempt to test the CME in a table-top experiment in a way similar to the quantum Hall effect. The biggest difference between the CME and the Hall effect arises from the fact that the carriers of electric charge are not the ordinary particles but the chirality; that is the excess of the right-handed particle number to the left-handed particle number [12]. It is quite non-trivial how to implement such a chiral battery (usually represented by $\mu_5 \neq 0$) in materials. Just recently the CME may have been confirmed in a system rather similar to the glasma, in which chirality imbalance is imposed by background fields that break \mathcal{CP} symmetry [13].

Figure 1 illustrates the schematic view of the CME setup in the HIC and in the condensed matter exper-

iment. The parallel \mathbf{E} and \mathbf{B} (in the z direction in Fig. 1) form \mathcal{P} - and \mathcal{CP} -odd product $\mathbf{E} \cdot \mathbf{B}$, and the CME current j^y is induced in a direction perpendicular to \mathbf{E} , which is reminiscent to the Hall current j^x . (In this sense one can regard the CME as a 3D extension of the quantum Hall effect.) In the HIC E^z and B^z are Abelian projected chromo-electric and chromo-magnetic fields. In the sphaleron transition these fields are provided from the Abelian projected part of the sphaleron gauge configuration too. Although Fig. 1 pictures an idealized environment, we would not lose generality and can interpret this back to more realistic circumstances relevant for each physical problem.

Theory of the particle and current production: In this work we focus on the right-handed sector only and the current (net particle) density should be doubled (canceled) once the left-handed sector is taken into account. The right-handed Weyl fermion should satisfy the following equation of motion:

$$(i\sigma^\mu \partial_\mu - e\sigma^\mu A_\mu)\phi_R = 0 \quad (1)$$

with $\sigma^\mu = (1, \boldsymbol{\sigma})$. We can readily construct a complete set of plane-wave solutions of Eq. (1) for the asymptotic states where the interaction is turned off. In general a constant background A_μ may be coupled even without interaction. In the present work we set a gauge that makes $A_0 = 0$ for a technical reason. We can then write positive-energy particle solutions as $\phi_R = u_R(\mathbf{p}; \mathbf{A})e^{-ip \cdot x}$ with

$$u_R(\mathbf{p}; \mathbf{A}) = \left(e^{i\theta(\mathbf{p}_A)} \frac{\sqrt{|\mathbf{p}_A| + p_A^z}}{\sqrt{|\mathbf{p}_A| - p_A^z}} \right) \quad (2)$$

in a certain gauge [or a convention for the overall U(1) phase]. Here we defined $\mathbf{p}_{\pm A} \equiv \mathbf{p} \mp e\mathbf{A}$ and the phase factor is $e^{i\theta(\mathbf{p}_A)} = (p_A^x + ip_A^y)/\sqrt{(p_A^x)^2 + (p_A^y)^2}$. We can identify the anti-particle state from $\phi_{\bar{R}} = -i\sigma^2 \phi_R^*$, which leads to a relation: $u_{\bar{R}}(\mathbf{p}; \mathbf{A}) = u_R(-\mathbf{p}; \mathbf{A})$. In the same way we can find the negative-energy particle and anti-particle solutions with $\phi_{R/\bar{R}} = v_{R/\bar{R}}(\mathbf{p}; \mathbf{A})e^{+ip \cdot x}$, which results in $v_R(\mathbf{p}; \mathbf{A}) = -e^{-i\theta(\mathbf{p}_A)}u_R(\mathbf{p}; -\mathbf{A})$ and $v_{\bar{R}}(\mathbf{p}; \mathbf{A}) = -e^{-i\theta(\mathbf{p}_A)}u_R(-\mathbf{p}; -\mathbf{A})$. We note that $u_R(\mathbf{p}; \mathbf{A})$ and $v_{\bar{R}}(\mathbf{p}; \mathbf{A})$ have an energy $\pm|\mathbf{p}_A|$, while other two, $u_{\bar{R}}(\mathbf{p}; \mathbf{A})$ and $v_R(\mathbf{p}; \mathbf{A})$, have an energy $\pm|\mathbf{p}_{-A}|$.

For the problem of particle and anti-particle production we evaluate an amplitude for the transition from a negative-energy state (with momentum \mathbf{p} and vector potential \mathbf{A}) to a positive-energy state (with momentum \mathbf{q} and vector potential \mathbf{A}'), which we can explicitly express as

$$\begin{aligned} \beta_{\mathbf{q}, \mathbf{p}} &= \int d^3x \frac{u_{\bar{R}}^\dagger(\mathbf{q}_{A'})e^{i|\mathbf{q}_{A'}|x^0 + i\mathbf{q} \cdot \mathbf{x}}}{\sqrt{2|\mathbf{q}_{A'}|}} f_{-\mathbf{p}}(x^0, \mathbf{x}), \\ \bar{\beta}_{\mathbf{q}, \mathbf{p}} &= \int d^3x \frac{u_{\bar{R}}^\dagger(\mathbf{q}_{-A'})e^{i|\mathbf{q}_{-A'}|x^0 + i\mathbf{q} \cdot \mathbf{x}}}{\sqrt{2|\mathbf{q}_{-A'}|}} \bar{f}_{-\mathbf{p}}(x^0, \mathbf{x}) \end{aligned} \quad (3)$$

for the particles and the anti-particles, respectively. We here introduced new functions, $f_{\mathbf{p}}(x)$ and $\bar{f}_{\mathbf{p}}(x)$, as solutions of the particle and the anti-particle equations of motion satisfying the following negative energy boundary conditions:

$$\begin{aligned} f_{\mathbf{p}}(x) &\rightarrow \frac{v_R(\mathbf{p}_{-A})e^{i|\mathbf{p}_{-A}|x^0 - i\mathbf{p} \cdot \mathbf{x}}}{\sqrt{2|\mathbf{p}_{-A}|}}, \\ \bar{f}_{\mathbf{p}}(x) &\rightarrow \frac{v_{\bar{R}}(\mathbf{p}_A)e^{i|\mathbf{p}_A|x^0 - i\mathbf{p} \cdot \mathbf{x}}}{\sqrt{2|\mathbf{p}_A|}} \end{aligned} \quad (4)$$

for x^0 around the initial time in the past. It should be noted that the equation of motion for the anti-particle is not Eq. (1) but e is replaced with $-e$. Finally we can express the net particle number (i.e. the particle number minus the anti-particle number *in the right-handed sector*) as well as the spatial currents in the following manner:

$$\begin{aligned} J^0 &= e \int \frac{d^3\mathbf{q}}{(2\pi)^3} (|\beta_{\mathbf{q}}|^2 - |\bar{\beta}_{\mathbf{q}}|^2), \\ \mathbf{J} &= e \int \frac{d^3\mathbf{q}}{(2\pi)^3} \left(\frac{\mathbf{q}_{A'}}{|\mathbf{q}_{A'}|} |\beta_{\mathbf{q}}|^2 - \frac{\mathbf{q}_{-A'}}{|\mathbf{q}_{-A'}|} |\bar{\beta}_{\mathbf{q}}|^2 \right), \end{aligned} \quad (5)$$

where the amplitudes above are the ones integrated over all incoming momenta, i.e.,

$$|\beta_{\mathbf{q}}|^2 \equiv \int \frac{d^3\mathbf{p}}{(2\pi)^3} |\beta_{\mathbf{q}, \mathbf{p}}|^2, \quad |\bar{\beta}_{\mathbf{q}}|^2 \equiv \int \frac{d^3\mathbf{p}}{(2\pi)^3} |\bar{\beta}_{\mathbf{q}, \mathbf{p}}|^2. \quad (6)$$

We note that J^0 above is a formula equivalent to that as utilized in Ref. [14].

Simulation setup and results: We here consider pulsed fields approximated by step functions for a duration T . We choose the origin of the time so that we start solving Eq. (1) numerically from $t = 0$. Introducing a temporal profile function defined by

$$\epsilon(t) \equiv \begin{cases} 1 & (-T/2 \leq t - t_0 \leq T/2) \\ 0 & (t - t_0 < -T/2; t - t_0 > T/2) \end{cases}, \quad (7)$$

we can explicitly specify the electric and magnetic fields we consider here as

$$E^z(t) = E_0 \epsilon(t), \quad B^z(t) = B_{\parallel} \epsilon(t), \quad B^y(t) = B_{\perp} \epsilon(t). \quad (8)$$

This choice of the temporal profile is motivated based on the glasma dynamics in which both the external magnetic field and the chromo-fields decay within the same time scale of ~ 0.1 fm/ c . Theoretically speaking, to define the produced particle number uniquely, we should setup the asymptotic states where interaction is switched off. We also mention another possibility to prescribe the particle number in a transient state (mostly relying on an adiabatic approximation) as studied in Ref. [15], though we do not adopt it.

We should make it clear that we neglect the back-reaction from the fields sourced by the produced particles. Because we start the simulation with the initial condition with zero particle, this approximation is expected to hold well especially for our setup with pulsed fields. In principle our formulation can be upgraded to the classical statistical simulation containing back-reaction [16], but this would be very costly. The classical evolution suffices for our present purpose to figure the net particle production and associated CME current generation out.

Let us now go into the numerical parts. It is important to keep the reflection symmetry of axes in order to avoid non-vanishing currents due to lattice artifact. Thus, the spatial sites n^i (that gives $x^i = n^i a$ with the lattice spacing a) take an integral value from $-N_i$ to $+N_i$ for $i = x, y, z$. The spatial volume is therefore $(2N_x+1) \cdot (2N_y+1) \cdot (2N_z+1) \cdot a^3$. The corresponding momenta are discretized as $p^i a = 2\pi k^i / (2N_i + 1)$. We also note that we should impose the anti-periodic boundary condition to avoid the singularity at $|\mathbf{p}_A| = 0$ in Eq. (2), which means that k^i should take half integral values from $-N_i + 1/2$ to $+N_i + 1/2$. One might think that one could evade the numerical singularity by inserting a small regulator in the denominator like the $i\epsilon$ prescription. Such a naive treatment of the singularity completely fails, however, because it is this infrared singularity that is responsible for the axial anomaly, which is manifested in the representation by Berry's curvature [17, 18] (see also Ref. [19] for another formulation of the chiral kinetic theory).

If we integrate over all momenta, we cannot avoid picking up all contributions from the doublers and the net particle production should be absolutely zero because the axial anomaly is exactly canceled according to the Nielsen-Ninomiya theorem [20]. It is thus crucial to get rid of the doubler contributions properly. To this end we limit our momentum integration range to the half Brillouin zone only, i.e., k^i from $-N_i/2 + 1/2$ to $+N_i/2 - 1/2$ (which is used in Ref. [14] too). We note that the axial anomaly is correctly captured from the singular contributions in the wave-function around $|\mathbf{p}_A| = 0$, though it usually appears near the ultraviolet cutoff in a diagrammatic approach. (We have numerically checked that our results are robust against small shifts at the momentum edges, which is also understandable from Fig. 2; produced particles are centered with small momenta. A relation to the conventional derivation of the CME formula involves subtle discussions, and we will address them in details in a separate publication.) One should not be confused with the situation in Euclidean, i.e., static lattice simulation in which the whole Dirac determinant should be evaluated to identify the statistical weight for gauge configurations.

In this work we choose a reference lattice size as $N_x = N_y = N_z = 8$ and scale physical quantities such as $E_0(N_i) = E_0(N_x = N_y = N_z = 8) \times 17^3 / [(2N_x + 1)(2N_y + 1)(2N_z + 1)]$ with varying N_i . To simplify no-

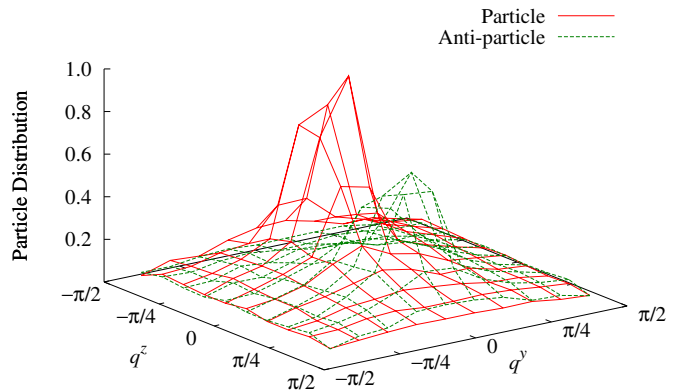


FIG. 2. Distribution of the produced particles and anti-particles as functions of q^y and q^z (and integrated with respect to q^x ; see the text). The lattice size is $N_x = N_y = N_z = 12$ and the magnetic fields are $B_{\parallel} = B_{\perp} = E_0/2$.

tation let us absorb e in the field definition and discard a hereafter. Then, we take: $E_0(N_x = N_y = N_z = 8) = 0.1$ for the reference lattice size and change B_{\parallel} and B_{\perp} from 0 to E_0 . We set the duration as $T = \sqrt{10/E_0}$ (that is 10 for the reference lattice size) and the central time of the pulse as $t_0 = 20$. We continue solving Eq. (1) up to $t = 2t_0$ with time spacing $\Delta t = 0.1$ using the 2nd-order Runge-Kutta method (with which we carefully checked that the accuracy is good enough for our present simulation up to $t = 2t_0$).

We do not quantize the field strength unlike Ref. [21]. Actually we compared results with unquantized and quantized fields (in the unit of $2\pi/N_x N_y$ for B_z etc) and found that this would make only negligible difference. Because our calculation is classical for gauge fields, non-quantization of the field strength is not harmful to numerical results, and moreover, we do not have to impose a boundary condition for a given gauge configuration at the spatial edges. We also make another remark about our gauge choice: $A^x = B^y z - B^z y$, $A^y = 0$, and $A^z = -E^x t$. In this case $E^x \neq 0$ is induced with time-dependent \mathbf{B} , and we set $A^y = 0$ not to have unwanted E^y for the investigation of the CME current.

Even if $B_{\parallel} = B_{\perp} = 0$, a finite E_0 would induce the *pair* production of particles and anti-particles under the Schwinger mechanism (see Ref. [22] for a comprehensive review). Because we deal with Weyl fermion, the pair production is always possible for any $E_0 \neq 0$, which leads to the distribution of particles with $p^z = 0 \sim -E_0 T$ and $p^x = p^y = 0$ (and with $p^z = 0 \sim +E_0 T$ for anti-particles). If B_{\parallel} or B_{\perp} is finite, this distribution is smeared in momentum space as clearly observed in Fig. 2 in which we present $\int (dq^x/2\pi) |\beta_q|^2$ and $\int (dq^x/2\pi) |\beta_q|^2$ as functions of q^y and q^z in the case with $B_{\parallel} = B_{\perp} = E_0/2$. In addition to smearing, it is evident in Fig. 2 that the particle is more enhanced over the anti-particle because of the \mathcal{CP} -odd background, which signals for the *net* production of

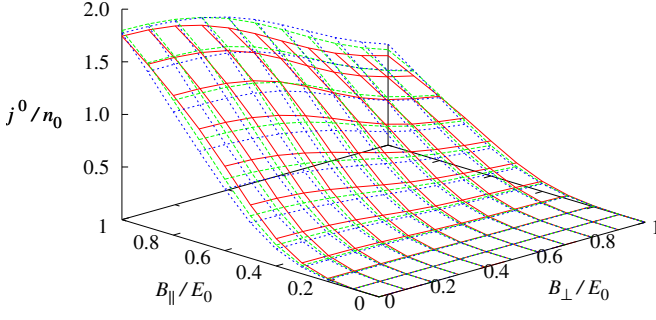


FIG. 3. Net particle density j^0 normalized by n_0 in Eq. (9) as a function of B_{\parallel} and B_{\perp} . The lattice size is $N_x = N_y = N_z = 8, 10, 12$ from the bottom (solid) to the top (dotted).

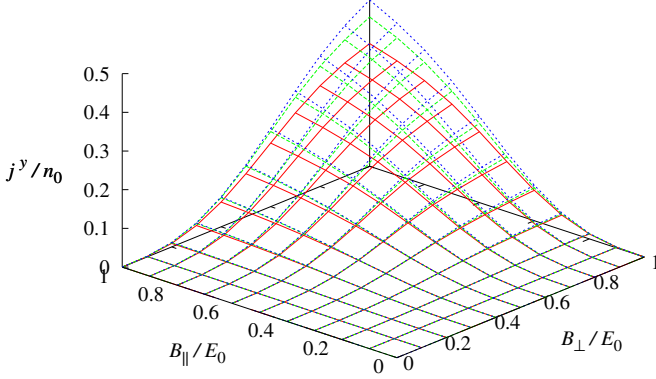


FIG. 4. Net current density j^y normalized by n_0 which is to be interpreted as the CME current.

right-handed particles. (For the vector gauge theory the total particle number is conserved with right-handed and left-handed contributions.)

In what follows we normalize $j^0 = J^0/V$ and $\mathbf{j} = \mathbf{J}/V$ by the number density:

$$n_0 = \frac{E_0^2}{4\pi^3} \cdot T, \quad (9)$$

which is the pair production rate $E_0^2/4\pi^3$ in the Schwinger mechanism multiplied by the duration T , which gives us an order-of-magnitude estimate. Then, j_0/n_0 should remain around $\sim \mathcal{O}(1)$, which is the case as confirmed in Fig. 3.

Figure 3 clearly evidences for a non-zero value of the net particle production for $\mathbf{E} \cdot \mathbf{B} = E_0 B_{\parallel} \neq 0$. We can make it sure that the net particle production is vanishing when $B_{\parallel} = 0$. This should be trivially so but a non-symmetric treatment of coordinates would pick up unphysical artifact, which is not the case in the present simulation. In Fig. 3 the lattice size is $N_x = N_y = N_z = 8, 10, 12$ from the bottom (solid) to the top (dotted). We can conclude that N_i dependence is mild.

Now we are going to discuss \mathbf{j}/n_0 obtained in our numerical calculation. Here let us focus only on the chiral magnetic current j^y and postpone discussions about the

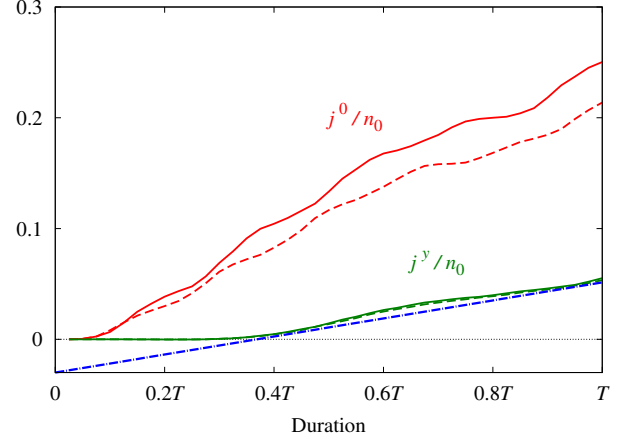


FIG. 5. Temporal profile of j^0 and j^y normalized by n_0 . The lattice size is $N_x = N_y = N_z = 12$ for solid lines and 14 for dashed lines. The magnetic fields are chosen as $B_{\parallel} = B_{\perp} = E_0/2$. The dashed-dotted line represents the current generation rate obtained analytically (with an offset by -0.03).

Hall current j^x and Ohm's current j^z to a longer paper with full details [23]. It is interesting that our results in Fig. 4 surely describe non-zero CME current as theoretically expected. We see that $j^y = 0$ when either B_{\parallel} or B_{\perp} is vanishing. Because j^y is the CME current, it is naturally vanishing if $B_{\perp} = 0$. Furthermore, $B_{\parallel} = 0$ means $\mathbf{E} \cdot \mathbf{B} = 0$, and so no net particle (or carrier) production is allowed (even though the pair production is possible as long as $\mathbf{E} \neq 0$). The current is vanishing then due to the lack of electric carrier. We can perceive from Fig. 4 that the lattice size dependence is slightly worse than the density in Fig. 3 but still mild.

It would be of paramount use in practice to consider j^0 and j^y as a function of the pulse duration. So far we fixed it as $T = \sqrt{10/E_0}$ and let us vary it then. Theoretically speaking, for a sufficiently large duration, we should expect linear dependence assuming a constant rate of particle production and current generation. In contrast, for a small duration, it is very difficult to predict what should happen *a priori*, and this is why we need numerical simulations.

Our numerical results in Fig. 5 (for $N_x = N_y = N_z = 12$ and 14 with $B_{\parallel} = B_{\perp} = E_0/2$) confirm nearly linear dependence for large durations (apart from small oscillation which is characteristic to magnetic phenomena). Although j^0 shows the lattice-size dependence, two results for j^y with different N_i 's are nearly overlaid to each other. For small durations, on the other hand, they exhibit a region of delay in which j^0 and j^y remain almost vanishing. The presence of such delay is intuitively understandable: it should take some time for the wave-function to transform from the free plane wave to the Landau-quantized one after a sudden switch-on of the magnetic field. We

would emphasize that what is quite non-trivial in Fig. 5 is that the delay for j^y is more than three times larger than that for j^0 . This fact should deserve more quantitative investigations: a longer delay would decrease a chance for the CME to be detected in the HIC. A systematic survey on this issue will be reported elsewhere [23]. Finally we draw an attention to the fact that our CME current j^y barely has lattice-size dependence and its slope (i.e. the current generation rate $\partial_t j^y$) agrees very well with the analytical estimate in Ref. [11].

Summary and outlook: We formulated the production of particles and anti-particles and checked its validity by looking for a right-handed particle excess in a \mathcal{CP} -odd domain. We limited our main concern to the CME current at present, but this type of the calculation should be applicable for a wider range of physical problems. For example, the (pair) particle creation at the horizon of the acoustic blackhole (see Ref. [24] for a pedagogical article) attracts attention, and it would be feasible to combine it with \mathcal{CP} -odd (or \mathcal{T} irreversible) background effects, for which we can apply our method. Of course, as mentioned in the beginning, possible applications should cover problems of sphaleron transitions in the electroweak and the strong interactions.

Here we emphasize the impact of the agreement between our numerical results and the analytical anticipations. It is very non-trivial that a direct evaluation of the current according to Eq. (5) could be consistent with quantum anomaly. Also we emphasize the importance of real-time character of the chiral magnetic current generation. The physical interpretation and the theoretical estimate of μ_5 are quite problematic and sometimes misleading in the literature. Our successful simulation is the first step toward a reliable quantification of initial μ_5 in HIC.

In this kind of approach to solve the equation of motion, the anomaly arises from the infrared singularity around $|\mathbf{p}_A| = 0$. The would-be lattice artifact might be attributed to underestimating the singular contributions there with coarse mesh. This implies that there may be a hybrid way to extract the singular terms analytically and to calculate non-singular parts numerically. This would reduce the lattice-size dependence and we can make theoretical estimates with improved reliability. Though we have confirmed that our CME current is close to the one in the continuum limit, it would be worth developing such a hybrid algorithm. Another direction for the improvement is to include back-reaction from gauge fluctuations. Once the back-reaction is taken into consideration, it would capture the effect of the chiral plasma instability [25]. Our progress in these directions will be

reported in a follow-up publication [23].

This work was partially supported by JSPS KAKENHI Grant Number 24740169.

-
- [1] F. R. Klinkhamer and N. S. Manton, Phys. Rev. D **30**, 2212 (1984).
 - [2] M. Yoshimura, Phys. Rev. Lett. **41**, 281 (1978) [Erratum-ibid. **42**, 746 (1979)].
 - [3] M. Fukugita and T. Yanagida, Phys. Lett. B **174**, 45 (1986).
 - [4] P. B. Arnold and L. D. McLerran, Phys. Rev. D **37**, 1020 (1988).
 - [5] L. D. McLerran, E. Mottola and M. E. Shaposhnikov, Phys. Rev. D **43**, 2027 (1991).
 - [6] D. Kharzeev, R. D. Pisarski and M. H. G. Tytgat, Phys. Rev. Lett. **81**, 512 (1998).
 - [7] D. E. Kharzeev, L. D. McLerran and H. J. Warringa, Nucl. Phys. A **803**, 227 (2008).
 - [8] K. Fukushima, D. E. Kharzeev and H. J. Warringa, Phys. Rev. D **78**, 074033 (2008).
 - [9] D. Kharzeev, A. Krasnitz and R. Venugopalan, Phys. Lett. B **545**, 298 (2002).
 - [10] Y. Hirono, T. Hirano and D. E. Kharzeev, arXiv:1412.0311 [hep-ph].
 - [11] K. Fukushima, D. E. Kharzeev and H. J. Warringa, Phys. Rev. Lett. **104**, 212001 (2010).
 - [12] D. Kharzeev and H.-U. Yee, Phys. Rev. **B88**, 115119 (2013).
 - [13] Q. Li, D. Kharzeev, C. Zhang *et al.*, arXiv:1412.6543 [cond-mat.str-el].
 - [14] F. Gelis, K. Kajantie and T. Lappi, Phys. Rev. C **71**, 024904 (2005); Phys. Rev. Lett. **96**, 032304 (2006).
 - [15] N. Tanji, Annals Phys. **324**, 1691 (2009); Annals Phys. **325**, 2018 (2010).
 - [16] F. Hebenstreit, J. Berges and D. Gelfand, Phys. Rev. Lett. **111**, 201601 (2013); V. Kasper, F. Hebenstreit and J. Berges, Phys. Rev. D **90**, 025016 (2014).
 - [17] D. T. Son and N. Yamamoto, Phys. Rev. Lett. **109**, 181602 (2012); Phys. Rev. D **87**, no. 8, 085016 (2013).
 - [18] M. A. Stephanov and Y. Yin, Phys. Rev. Lett. **109**, 162001 (2012).
 - [19] J. H. Gao, Z. T. Liang, S. Pu, Q. Wang and X. N. Wang, Phys. Rev. Lett. **109**, 232301 (2012); J. W. Chen, S. Pu, Q. Wang and X. N. Wang, Phys. Rev. Lett. **110**, no. 26, 262301 (2013).
 - [20] H. B. Nielsen and M. Ninomiya, Phys. Lett. B **105**, 219 (1981).
 - [21] G. S. Bali, F. Bruckmann, G. Endrodi, Z. Fodor, S. D. Katz, S. Krieg, A. Schafer and K. K. Szabo, JHEP **1202**, 044 (2012).
 - [22] G. V. Dunne, In *Shifman, M. (ed.) et al.: From fields to strings, vol. 1* 445-522.
 - [23] K. Fukushima and P. Morales, in preparation.
 - [24] R. Balbinot and A. Fabbri, Adv. High Energy Phys. **2014**, 713574 (2014).
 - [25] Y. Akamatsu and N. Yamamoto, Phys. Rev. Lett. **111**, 052002 (2013); Phys. Rev. D **90**, no. 12, 125031 (2014).